SC5271.6SA

Copy No. 16

NUMERICAL METHODS FOR 2-DIMENSIONAL PROCESS MODELING

W.D. Murphy and W.F. Hall
Rockwell International Science Center
P.O. Box 1085
Thousand Oaks, California 91360

and

C.D. Maldonado
Rockwell International Microelectronics R&D Center
3370 Miraloma Avenue
Anaheim, California 92803

July, 1981

Semi Annual Technical Report No. 2
for Period 1 January 1981 - 30 June 1981

Approved for public release; distribution unlimited

The views and conclusions contained in this document are those of the authors and should not be interpreted as representing the official policies, either expressed or implied, of the Defense Advanced Research Projects Agency of the U.S. Government.

Sponsored by

Defense Advanced Research Projects Agency (DoD)
DARPA Order No. 3984
Under Contract No. MDA903-80-C-0498
Issued by
Department of the Army, Defense Supply Service-Washington
Washington, D.C. 20310

Rockwell International
Science Center

UNCLASSIFIED

SECURITY CLASSIFICATION OF THIS PAGE (When Data Entered)

REPORT DOCUMENTATION PAGE

READ INSTRUCTIONS BEFORE COMPLETING FORM

1. REPORT NUMBER

2. GOVT ACCESSION NO. AD-A102 847

3. RECIPIENT'S CATALOG NUMBER

4. TITLE (and Subtitle) (6)
NUMERICAL METHODS FOR 2-DIMENSIONAL PROCESS MODELING.

5. TYPE OF REPORT & PERIOD COVERED
Semi-Annual Technical Report
01/01/81 – 06/30/81

6. PERFORMING ORG. REPORT NUMBER (14)
SC5271.6SA

7. AUTHOR(s) (10)
W.D. Murphy, W.F. Hall[redacted] C.D. Maldonado

8. CONTRACT OR GRANT NUMBER(s) (15)
MDA903-80-C-0498
~DARPA Order-3984

9. PERFORMING ORGANIZATION NAME AND ADDRESS
Rockwell International Science Center
P.O. Box 1085
Thousand Oaks, California 91360

10. PROGRAM ELEMENT, PROJECT, TASK AREA & WORK UNIT NUMBERS
DARPA Order No. 3984

11. CONTROLLING OFFICE NAME AND ADDRESS (11)
Defense Advanced Research Project Agency
1400 Wilson Boulevard
Arlington, Virginia 22209 (TIO/Admin.)

12. REPORT DATE
Jul[redacted]81 (12) 42

13. NUMBER OF PAGES
38

14. MONITORING AGENCY NAME & ADDRESS(if different from Controlling Office)
Department of the Army
Defense Supply Service-Washington
Washington, D.C. 20310

15. SECURITY CLASS. (of this report)
Unclassified

15a. DECLASSIFICATION/DOWNGRADING SCHEDULE

16. DISTRIBUTION STATEMENT (of this Report)
Approved for public release; distribution unlimited

(9) Semi-annual technical rept. no. 2, 1 Jan-30 Jun 81,

17. DISTRIBUTION STATEMENT (of the abstract entered in Block 20, if different from Report)

18. SUPPLEMENTARY NOTES

19. KEY WORDS (Continue on reverse side if necessary and identify by block number)
very large scale integration (VLSI), diffusion, solid state, electron devices

20. ABSTRACT (Continue on reverse side if necessary and identify by block number)
The completion and testing of a fast algorithm for the calculation of two-dimensional dopant redistribution during oxide growth is described. A numerical comparison with analytical, exact solutions for low-dose implants is made which shows negligible error.

DD FORM 1 JAN 73 1473 EDITION OF 1 NOV 65 IS OBSOLETE

UNCLASSIFIED

SECURITY CLASSIFICATION OF THIS PAGE (When Data Entered)

389949 not

CONTENTS

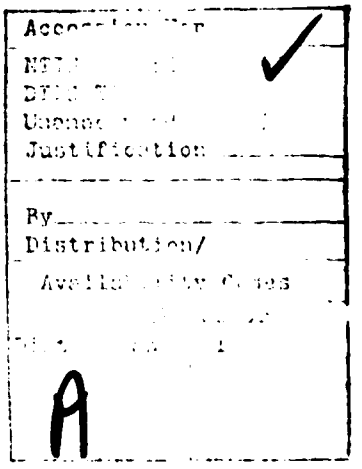

ILLUSTRATIONS

1.0 SUMMARY

This technical report presents the results of the second six months of research on numerical methods for two-dimensional process modeling under Contract MDA903-80-C-0498, DARPA Order No. 3984. During the first six months of the contract effort, a fast algorithm for computing dopant spread was found and tested. In the current period, a code incorporating nonuniform motion of the oxide-silicon boundary was written around this algorithm, and tests were made on typical process conditions which showed that the most difficult process steps, involving simultaneous nonuniform oxide growth and nonlinear dopant diffusion, could be accurately simulated in under 30 seconds of CPU time on the Cyber 176. Transfer of the basic algorithm to the process and device modeling group at Stanford has been initiated. In addition, the capabilities of this algorithm were reviewed at the Second International Conference on Numerical Analysis for Semiconductor Devices and Integrated Circuits, held in Dublin, Ireland, June 17-19, 1981.

1.1 TASK OBJECTIVES

The overall objective of this program is to develop fast and accurate methods for computer modeling of the two-dimensional spread of dopants and other defects during VLSI circuit fabrication. Our initial goals have been to demonstrate these methods for nonlinear diffusion of a single dopant during oxide growth, and to provide the resulting computational algorithms in a form suitable for

incorporation into a general process modeling computer code, such as Stanford's program SUPREM.

Three tasks were defined for the first year's effort:

Task 1 – Analysis of Numerical Methods

Task 2 – Formulation of Test Cases

Task 3 – Algorithm Development and Evaluation .

Their objectives are, respectively:

Task 1 – Select promising algorithms from other disciplines, primarily fluid dynamics, where considerable progress on numerical methods for multidimensional problems has recently been made.

Task 2 – a) Determine realistic parameter ranges to be used as test cases for source and drain diffusion into a short MOSFET channel region.

b) Develop and analyze two-dimensional diffusion problems for which dopant profiles can be obtained to high accuracy by existing techniques.

Task 3 – a) Evaluate each selected algorithm for speed and accuracy.

b) Adapt the most promising algorithm(s) to solve the combined oxidation-nonlinear diffusion problem for a single dopant species in two dimensions.

All objectives of the first year's effort have been accomplished.

The specific objectives for the second year include:

1. Effective transfer of the basic algorithm to the integrated circuits community;
2. Extension of the code to treat multiple interacting species and three-dimensional redistribution; and
3. Exploration of the computational requirements posed by better physical models for the underlying processes of chemical reaction and defect generation and migration.

Much of the groundwork for accomplishing the first two objectives has already been laid. A computer code incorporating the basic algorithm and providing user interface routines adapted from *SUPREM* is in the final stages of documentation, and is presently scheduled for delivery to Stanford in August. It will also be available directly to interested users. With regard to multiple species and three-dimensional redistribution, only the addition of subroutines to the existing code will be required, as the basic algorithm is already set up to handle the more general cases.

1.2 TECHNICAL PROBLEM

The fabrication of VLSI devices requires production of features of submicron size and separation. Electrical characteristics such as threshold and punchthrough voltages will be sensitive to dopant spread into critical areas adjacent to the original features. Experimental control of this spreading, without guidance from accurate computer

modeling, will be costly, tedious, and time-consuming. However, the use of standard numerical methods to achieve an adequate modeling capability is also costly and time-consuming. One should therefore seek advanced methods, drawn from areas such as fluid dynamics, where considerable effort and ingenuity have been expended in recent years to develop fast and accurate solvers for the characterization of multidimensional, time-dependent phenomena.

1.3 GENERAL METHODOLOGY

Based upon our own ongoing research in computational nonlinear aerodynamics, we identified several promising approaches to the development of a fast solver for two-dimensional diffusion problems. After a preliminary screening, a few of these were selected for adaptation to the problem of dopant spread during oxidation or annealing. These algorithms were tested for speed and accuracy on the problem of nonlinear dopant diffusion into the channel region of a MOSFET, as well as on simpler problems for which the actual dopant profiles could be accurately obtained by other means.

1.4 TECHNICAL RESULTS

The principal technical result obtained during the second six months of contract effort was the successful incorporation of nonuniform oxide growth into the dopant redistribution code. Typical process steps involving implant redistribution in the vicinity of a growing bird's beak field oxide have been run in under 30 seconds on the

Cyber 176 (see Appendix). Given computer times of this order, the iterative use of this code to design a fabrication process in two dimensions, much as SUPREM is used in one dimension, now appears practical.

Additional results worthy of note are the verification of accuracy for the method of lines algorithm, reported in Section 2 below, and a comparison of those factors which dominate the time and storage requirements for this algorithm, and for the finite-element algorithm now in common use for solving the partial differential equations encountered in process and device simulation, given in the Appendix.

1.5 IMPORTANT FINDINGS AND CONCLUSIONS

The first year's effort has produced a fast and accurate algorithm which handles an essential part of the VLSI process simulation problem: dopant spread in two dimensions during annealing or nonuniformly oxidizing process steps. Its speed is sufficiently high to encourage iterative use by the process engineer in selecting process parameters for those steps. While the code should be useful in its present form, which includes user interface routines adapted from SUPREM, it is intended to function within the framework of a complete, two-dimensional process simulator. By providing this code to the Stanford modeling group, we hope to stimulate the creation of such a simulator. Alternatively, process design groups presently engaged in VLSI fabrication can utilize the code as it stands.

1.6 SPECIAL COMMENTS

As part of the strategy to achieve effective transfer of our results to the integrated circuits community, we are

publicizing the capabilities of the algorithm. A short paper on this subject was presented in June at the Second International Conference on Numerical Analysis of Semiconductor Devices and Integrated Circuits, and another is scheduled for the 1981 Symposium on VLSI Technology this September. Copies of these papers are included in the Appendix to this report. Judging from the response to our first presentation, there will be a number of groups requesting copies of the code and the associated documentation in the near future. Representatives from Honeywell, IBM, Phillips, Thomson-EFCIS, and others have already expressed interest.

1.7 IMPLICATIONS FOR FURTHER RESEARCH

One essential advantage of the basic algorithm can be stated as follows: Both time and storage requirements grow only as the number of unknowns in the problem. This implies that introducing a second dopant will, for a fixed mesh, only double the CPU time, or that treating dopant spread into a third dimension will multiply this time by the number of intervals chosen along this dimension. It thus appears that the planned extensions to these more complex process conditions will not place excessive demands on the computer.

The growing availability of parallel-architectured computers such as the CDC 205 and the Cray series presents the interesting possibility of achieving a large increase in the speed of the basic algorithm. The iterative solution process which dominates the computer time can be recast to take advantage of both pipeline structure and simultaneous,

independent arithmetic operations. Such a gain in speed could bring the investigation of detailed multiple defect models within the scope of routine computer analysis on parallel machines.

2.0 CORRELATION WITH ANALYTICAL PREDICTIONS

In this section, numerical simulations for the thermal redistribution of 40 keV boron and arsenic implants are correlated with analytical predictions. These simulations were carried out for low dose ($5 \times 10^{11}\,cm^{-2}$) implants so the governing diffusion equation is linear. Also, the problem was further simplified by utilizing a non-oxidizing ambient to drive the implants into the bulk of the silicon medium. For drive-in problems, the simplification of the boundary value problem arises from the fact that the boundaries are stationary. Figure 1 is a qualitative two-dimensional sketch for defining the drive-in boundary value problem. In this figure a window, $y \leq |a|$, has been etched out of an impenetrable mask along the z direction. Through this window, an implant is introduced into the silicon medium via a thin ($\sim$ 0.005 μm) protective oxide (SiO_2) pad. On entering the silicon medium, the implant will be distributed two dimensionally as follows:[1]

$$N(x,y,0) = \frac{N_d \times 10^4}{2\sqrt{2\pi}\,\sigma_p} \exp\left[-\frac{(x-\tilde{R}_p)^2}{2\sigma_p^2}\right] \left\{ \operatorname{erf}\left[\frac{(y+a)}{\sqrt{2}\,\sigma_L}\right] - \operatorname{erf}\left[\frac{(y-a)}{\sqrt{2}\,\sigma_L}\right] \right\} (cm^{-3}) \,, \qquad (1)$$

where N_d is the dose in cm^{-2}, $\tilde{R}_p = R_p - U_o$, U_o is the oxide pad thickness, R_p is the projected range, and σ_p and σ_L are the vertical and lateral standard deviations, respectively.

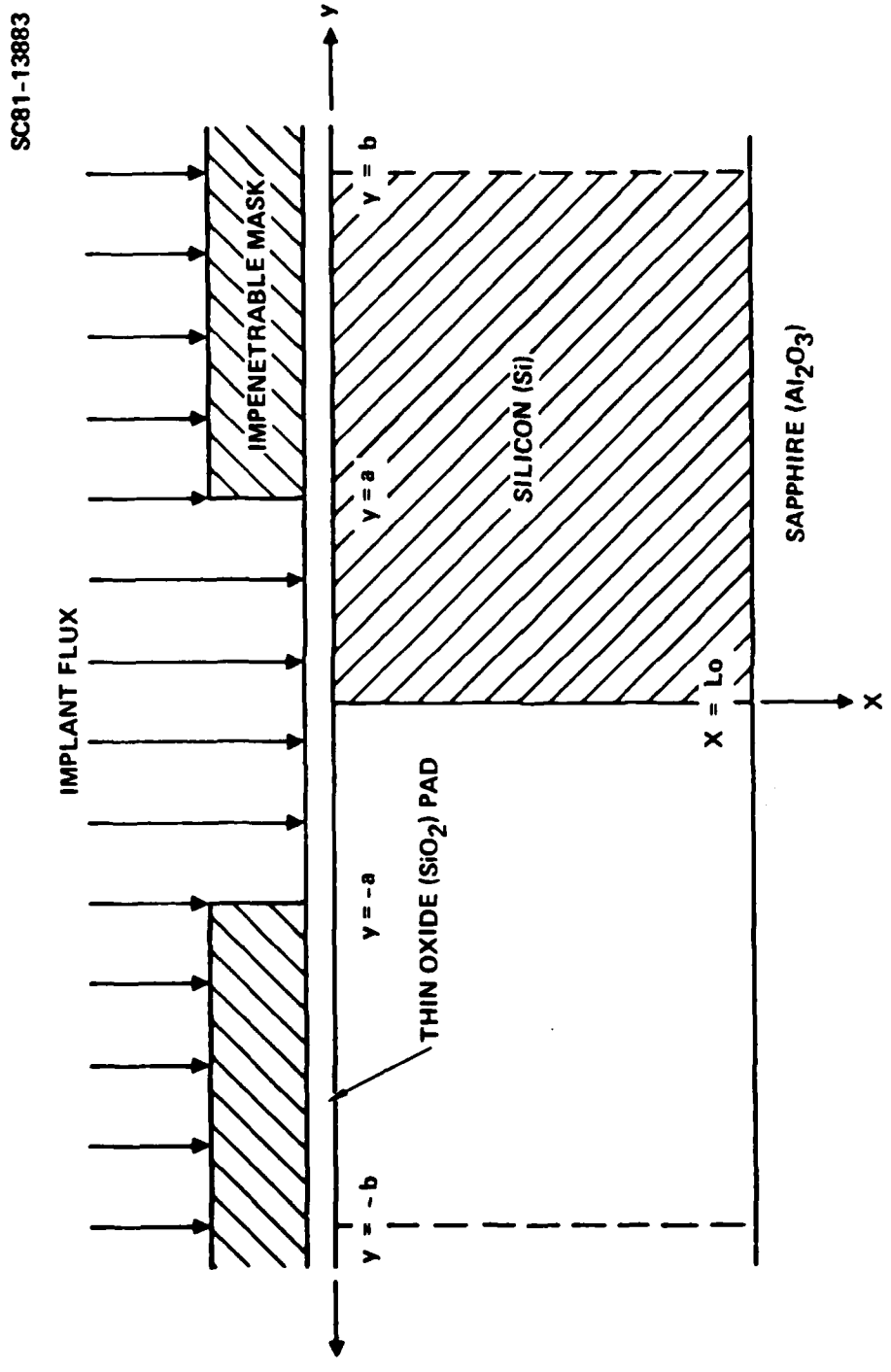

Fig. 1. Qualitative two-dimensional geometrical sketch for defining the drive-in boundary value problem.

When the window is brought into contact with a non-oxidizing ambient, the implant distribution given by Eq. (1) will be thermally driven-in. The governing equation for the redistribution of impurities is obtained on combining the continuity equation with Fick's law[2] for the impurity flux density vector. This gives rise to the result,

$$\frac{\partial}{\partial x}\left[D\,\frac{\partial}{\partial x}\,N\right] + \frac{\partial}{\partial y}\left[D\,\frac{\partial}{\partial y}\,N\right] - \frac{\partial}{\partial t}\,N = 0\ , \tag{2}$$

where D is the diffusion coefficient, which is constant for low dose implants and concentration dependent for high dose implants. On the boundaries of the domain $\{0 \leq x \leq L_o,\ y \leq b\}$ of Fig. 1 on which Eq. (2) is defined, the impurity concentration satisfies the following conditions:

$$\frac{\partial}{\partial x}\,N\Big|_{x=0} = 0\ , \tag{3}$$

$$\frac{\partial}{\partial x}\,N\Big|_{x=L_o} = 0\ , \tag{4}$$

and

$$\frac{\partial}{\partial y}\,N\Big|_{y=\pm b} = 0\ . \tag{5}$$

The silicon-silicon dioxide and silicon-sapphire interfaces located at x=0 and $x=L_o$, respectively, are assumed to be impenetrable barriers to out diffusion, hence, Eqs. (3) and

(4) are strictly reflecting boundary conditions. The boundary conditions at y=±b and given by Eq. (5) imply that the structure shown in Fig. 1 repeats itself periodically in the lateral direction.

The solution to the boundary value problem defined by Eqs. (2) to (5) for a specified initial distribution as given by Eq. (1) can be obtained analytically for a constant diffusion coefficient, D, corresponding to low dose implants. This solution will be in the form of a double infinite series of damped two-dimensional trigonometric modes whose generalized Fourier coefficients must be evaluated numerically in terms of the specified initial distribution. Since this solution requires a considerable amount of programming effort in order to simulate the redistribution of drive-in impurity profiles on a computer, a simplification of the boundary value problem was considered. The simplified problem retains the boundary condition given by Eq. (3), but considers the silicon-sapphire interface and the lateral positions at y=±b to be remotely located so that no impurities are reflected from these boundaries. An excellent approximation to this latter problem involves the solution to Eq. (2) as an initial value problem with N(x,y,0) specified by Eq. (1), such that N(x,y,t) satisfies Eq. (3) for all values of time and natural boundary conditions, that is, both the impurity concentration and its derivatives vanish as the boundaries located at $x=L_o$ and y=±b recede to infinity. The solution to this problem is formally given as

$$N(x,y,t) = \int_{-\infty}^{+\infty} dy_o \int_0^{+\infty} dx_o N(x_o,y_o,0) G(x_o,y_o,0|x,y,t) \quad (6)$$

where the kernel under the integral, given explicitly by

$$G(x_o,y_o,0|x,y,t) = \frac{1}{4\pi Dt}\exp\left[-\frac{(y-y_o)^2}{4Dt}\right]\left\{\exp\left[-\frac{(x-x_o)^2}{4Dt}\right] + \exp\left[-\frac{(x+x_o)^2}{4Dt}\right]\right\}, \quad (7)$$

is the Green's function or impulse response; that is, it is the response at the field point, (x,y), for a time $t > 0$ due to an impulse of impurities which is introduced at the source point, (x_o,y_o), at time $t = 0$.

The introduction of Eqs. (1) and (7) into Eq. (6) for $N(x_o,y_o,0)$ and $G(x,y,t|x_o,y_o,0)$, respectively, yields

$$N(x,y,t) = \frac{2\cdot 10^4 \cdot N_d}{\pi^{3/2}\sqrt{2\sigma_p^2 + 4Dt}}\exp\left[-\frac{R_p^2}{2\sigma_p^2}\right]\exp\left[-\frac{x^2}{4Dt}\right]L(x)H(y) , \quad (8)$$

where

$$L(x) = \int_0^{+\infty} d\xi\ \exp(-\xi)\left\{\xi^{-\frac{1}{2}}\exp\left[\frac{\sqrt{4Dt}\,R_p\xi^{\frac{1}{2}}}{\sigma_p\sqrt{\sigma_p^2 + 2Dt}}\right]\cosh\left[\frac{2\sigma_p x\xi^{\frac{1}{2}}}{\sqrt{4Dt}\sqrt{\sigma_p^2 + 2Dt}}\right]\right\} \quad (9)$$

and

$$H(y) = \int_{-\infty}^{+\infty} d\eta\ \exp(-\eta^2)\left\{\mathrm{erf}\left[\frac{1}{\sqrt{2}\,\sigma_L}(y + a - \sqrt{4Dt}\eta)\right] - \mathrm{erf}\left[\frac{1}{\sqrt{2}\,\sigma_L}(y - a - \sqrt{4Dt}\eta)\right]\right\} . \quad (10)$$

L(x) and H(y) were evaluated numerically using the Gauss-Laguerre and Gauss-Hermite quadratures, respectively.

2.1 BORON IMPLANT

The initial spatial distribution of the boron implant as specified by Eq. (1), but with a uniform background of $N_b = 10^{15} cm^{-3}$ added to it, is plotted in Fig. 2. In carrying out the calculation based on Eq. (1), a window opening of 2a = 1 μm was assumed and the extreme lateral dimension of the domain, b, was set equal to 1.5 μm. The silicon film thickness, L_o, was chosen to be 1 μm. For a 40 keV boron implant, the projected range statistics of Ref. 3 yielded the following parameter values: $R_p = 0.1302$ μm, $\sigma_p = 0.0443$ μm, and $\sigma_L = 0.0682$ μm. The dose of the boron implant was low ($5 \times 10^{11} cm^{-2}$) so the redistribution problem is linear. In Fig. 2(a), the two-dimensional distribution is plotted only over the cross-hatched domain of Fig. 1 because y=0 is a plane of symmetry; while in Fig. 2(b), the equi-density contours are shown. Besides providing qualitative insight into the two-dimensional spatial distribution of the boron implant, Fig. 2 likewise provides information on the lateral penetration of the implant.

When the structure of Fig. 1 is brought in contact with an inert or nonoxidizing ambient, such as argon, the boron implant in Fig. 2 will be thermally redistributed. For an ambient temperature of 1000°C the diffusion coefficient, D, was set equal to the non-enhanced intrinsic value, 0.0055 $\mu m^2/hr$, for boron in silicon. The redistributed two-dimensional profile corresponding to a drive-in time

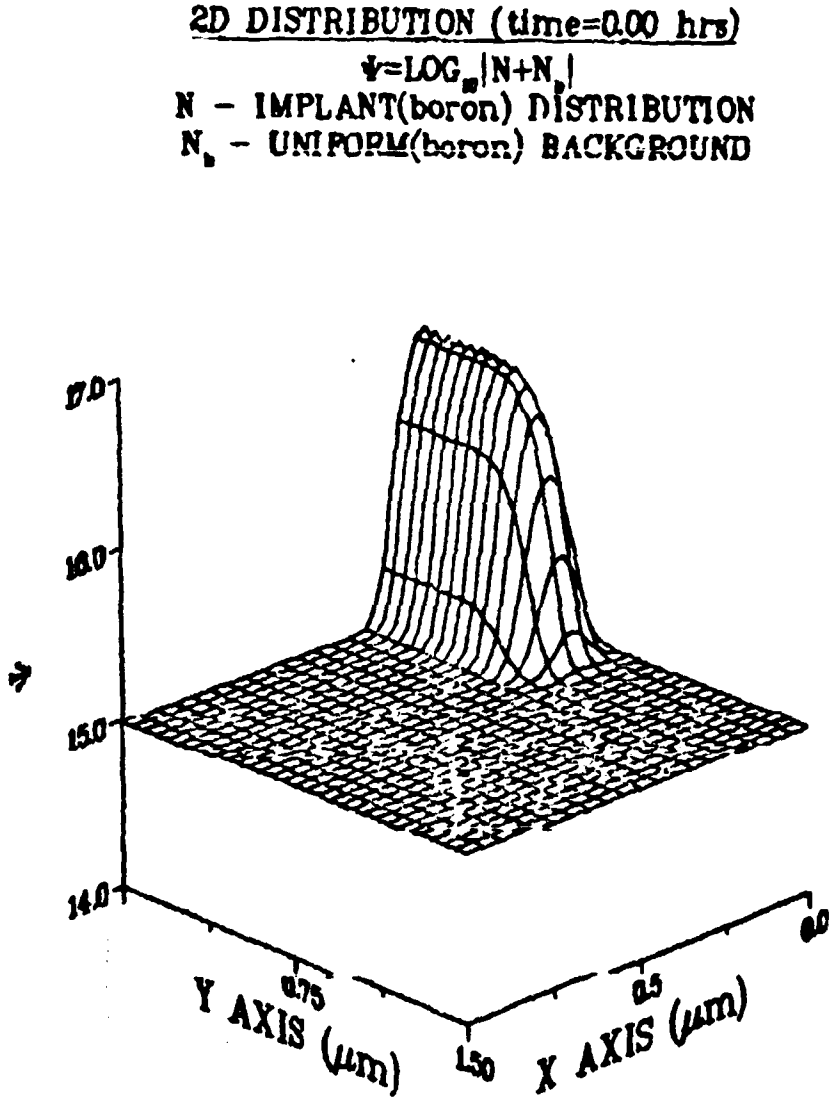

Fig. 2(a). Two-dimensional Furukawa distribution for a 40 keV boron implant of dose $5 \times 10^{11}\,cm^{-2}$.

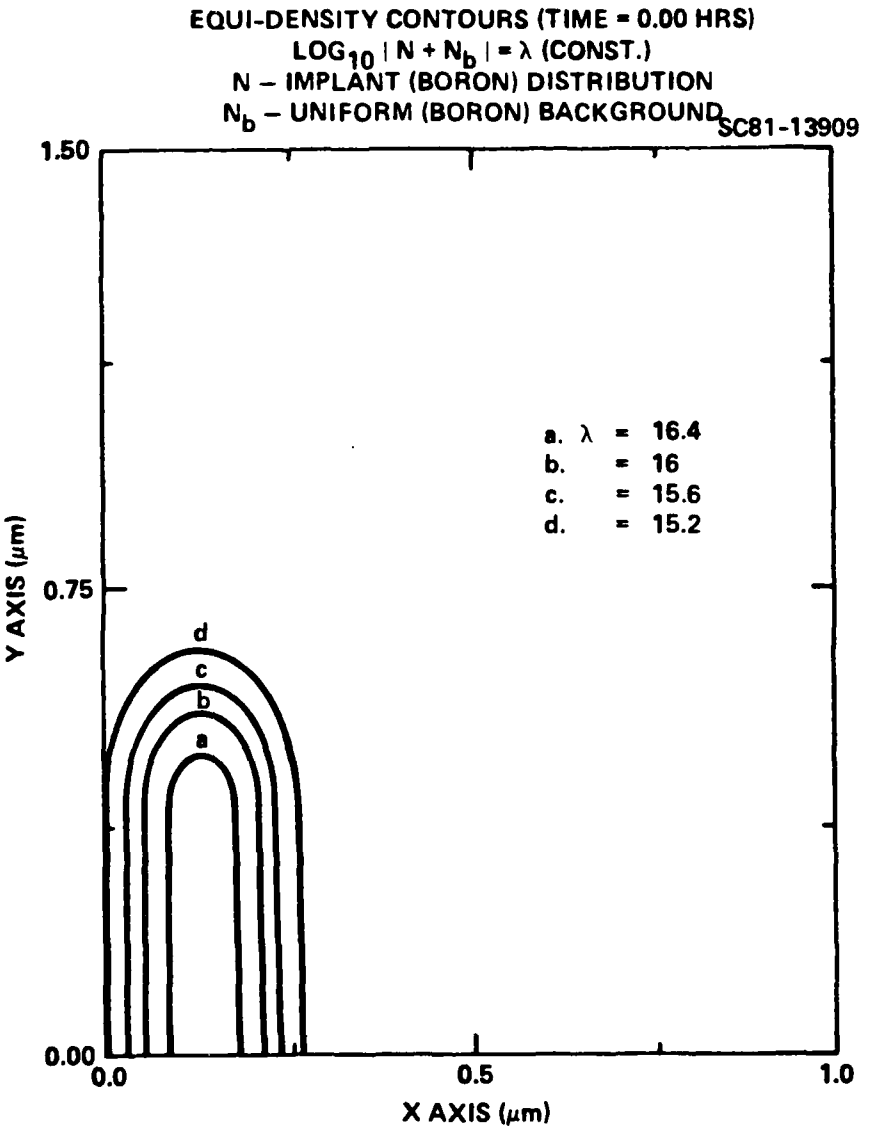

Fig. 2(b). The equi-density contours for Fig. 2(a).

of 1 hr is shown in Fig. 3. For the two-dimensional distribution shown in Fig. 3(a) and equi-density contours of Fig. 3(b), the cross-hatched computational domain in Fig. 1 was uniformly subdivided into a grid of 41 × 61 points and the solution at these grid points evaluated by Eq. (8). One-dimensional profiles along the x direction corresponding to y=0 (plane of symmetry) and y=a (edge of window) are shown in Fig. 4. These profiles are for the situation where the implant is decoupled from the background. The solid curves in Fig. 4 are the results predicted analytically by Eq. (8), while the open and solid circles are the results obtained numerically for the fine ($\Delta x = \Delta y = 0.0125$ μm) and coarse ($\Delta x = \Delta y = 0.05$ μm) partitions, respectively.

An inventory of the results shown in Fig. 4 reveals that from a qualitative viewpoint, the numerical results for both the coarse and fine partitions are in excellent agreement with the analytical results; however, the numerical results for the fine partition yielded the better correlation. Although the numerical results for the intermediate ($\Delta x = \Delta y = 0.025$ μm) partition are not plotted in Fig. 4, their quantitative correlation with the analytical results is shown in Table 1. An inventory of the results in Table 1 reveals that analytical and numerical solutions are in excellent agreement over the entire depth of the pertinent portion ($> 10^{15}\,cm^{-3}$) of the redistributed boron profile.

2.2 ARSENIC IMPLANT

The parameter values $R_p = 0.0269$ μm, $\sigma_p = 0.0099$ μm, and $\sigma_L = 0.0103$ μm, as obtained from Ref. 3, were utilized

2D DISTRIBUTION (time=1.00 hrs)

$\Psi = LOG_{10}|N+N_b|$

N - IMPLANT(boron) DISTRIBUTION

N_b - UNIFORM(boron) BACKGROUND

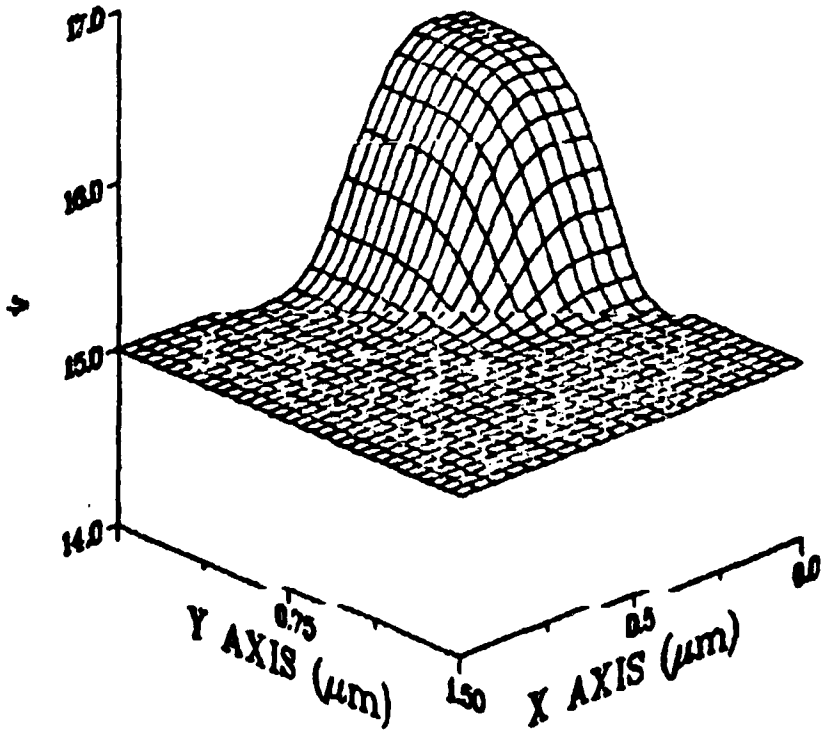

Fig. 3(a). Redistributed two-dimensional profile for the boron implant shown in Fig. 2 after 1 hr of drive-in time in an inert argon ambient at 1000°C.

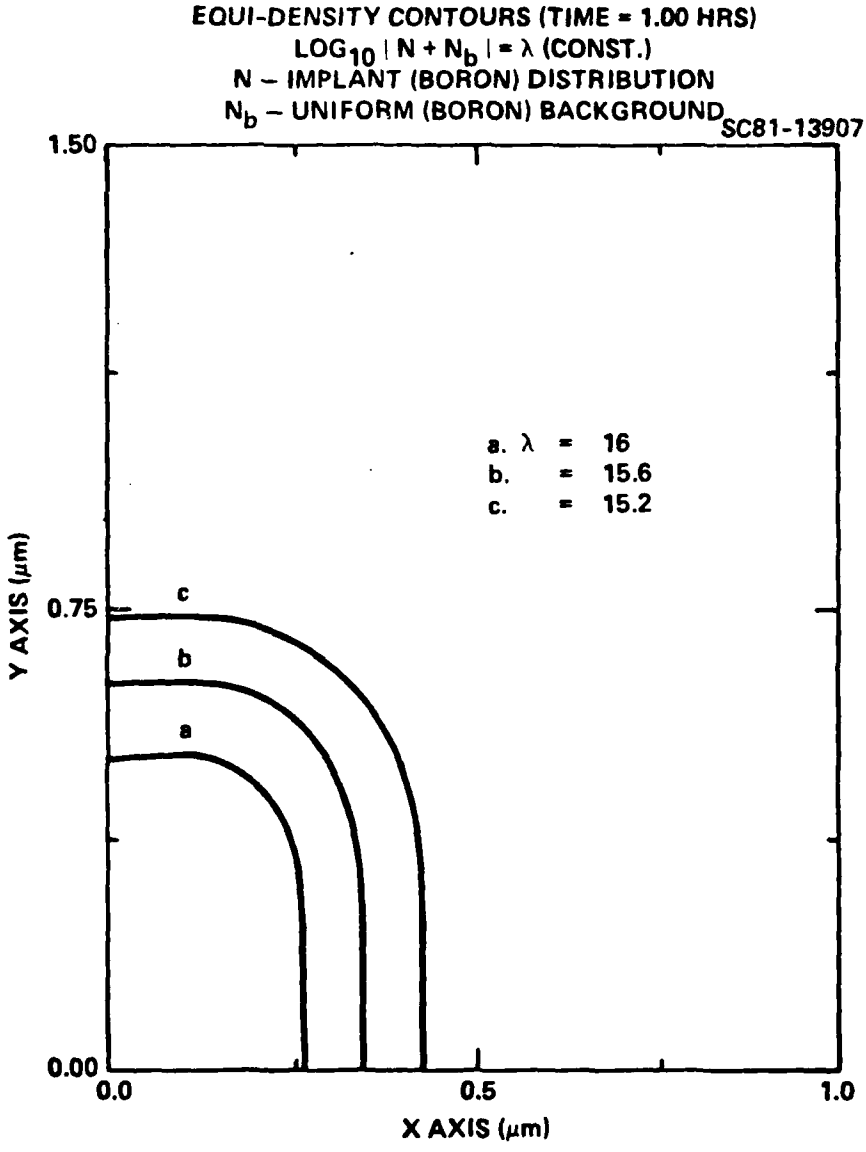

Fig. 3(b). The equi-density contours for Fig. 3(a).

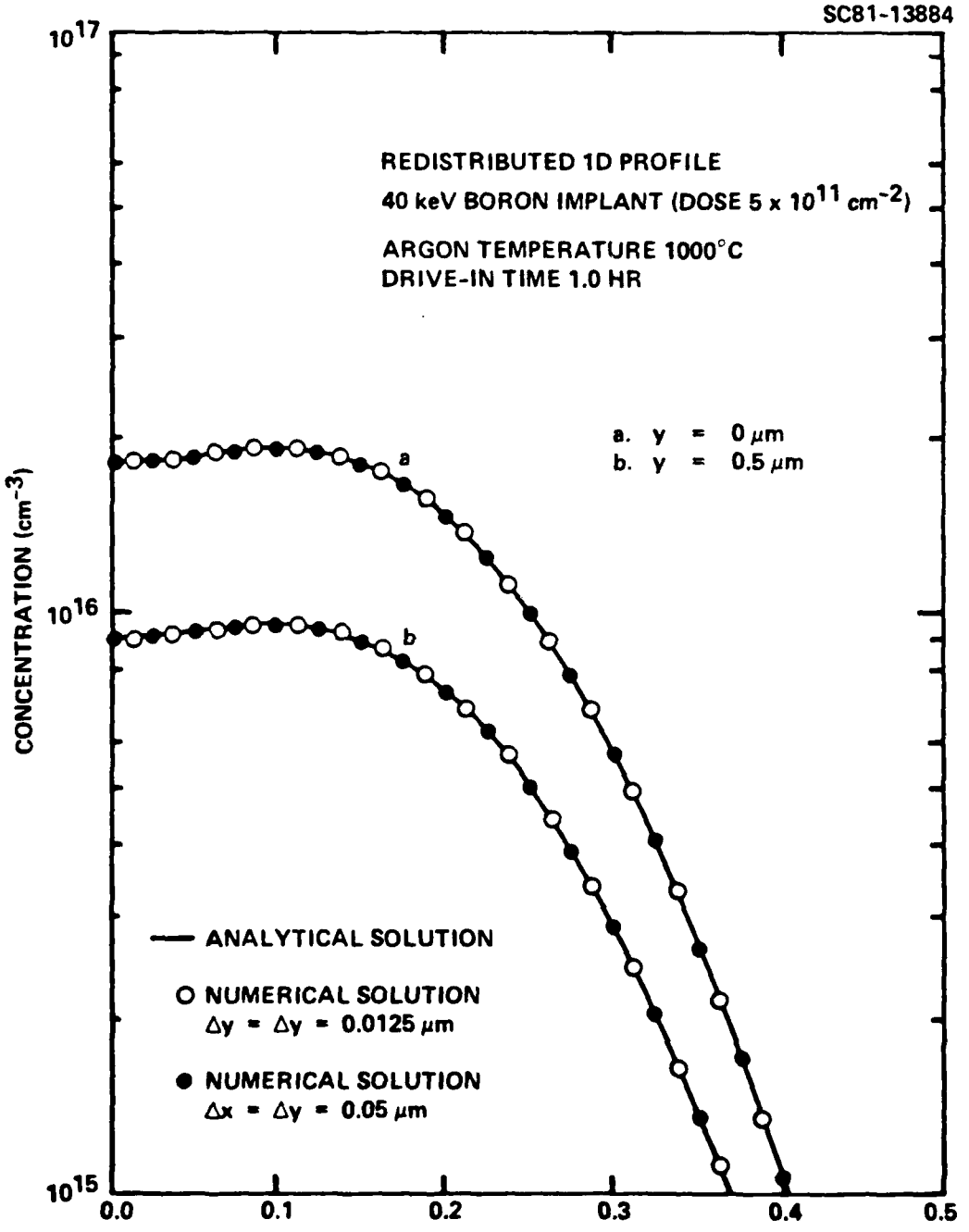

Fig. 4. Correlation of analytical and numerical predictions along the x direction for y=0 μm and y=0.5 μm (mask edge) for the distribution shown in Fig. 3 but with the redistributed implant decoupled from the background.

Table 1. Correlation of Numerical and Analytical Predictions for Boron Implant*

x Position (μm)	y = 0 μm			y = 0.5 μm (Mask Edge)		
	Numerical (cm^{-3})	Analytical (cm^{-3})	% Error	Numerical (cm^{-3})	Analytical (cm^{-3})	% Error
0	0.1805×10^{17}	0.1816×10^{17}	-0.61	0.9027×10^{16}	0.9080×10^{16}	-0.58
0.025	0.1820×10^{17}	0.1829×10^{17}	-0.49	0.9100×10^{16}	0.9146×10^{16}	-0.50
0.050	0.1856×10^{17}	0.1862×10^{17}	-0.32	0.9285×10^{16}	0.9311×10^{16}	-0.28
0.075	0.1897×10^{17}	0.1989×10^{17}	-0.05	0.9491×10^{16}	0.9491×10^{16}	0.00
0.100	0.1918×10^{17}	0.1914×10^{17}	+0.21	0.9595×10^{16}	0.9572×10^{16}	+0.24
0.125	0.1896×10^{17}	0.1889×10^{17}	+0.37	0.9484×10^{16}	0.9446×10^{16}	+0.40
0.150	0.1815×10^{17}	0.1808×10^{17}	+0.39	0.9082×10^{16}	0.9041×10^{16}	+0.45
0.175	0.1673×10^{17}	0.1668×10^{17}	+0.30	0.8372×10^{16}	0.8341×10^{16}	+0.37
0.200	0.1479×10^{17}	0.1477×10^{17}	+0.14	0.7400×10^{16}	0.7385×10^{16}	+0.20
0.225	0.1251×10^{17}	0.1252×10^{17}	-0.08	0.6256×10^{16}	0.6258×10^{16}	-0.03
0.250	0.1010×10^{17}	0.1013×10^{17}	-0.30	0.5051×10^{16}	0.5067×10^{16}	-0.32
0.275	0.7789×10^{16}	0.7832×10^{16}	-0.55	0.3894×10^{16}	0.3916×10^{16}	-0.56
0.300	0.5731×10^{16}	0.5774×10^{16}	-0.74	0.2865×10^{16}	0.2887×10^{16}	-0.76
0.325	0.4026×10^{16}	0.4059×10^{16}	-0.81	0.2012×10^{16}	0.2030×10^{16}	-0.89
0.350	0.2701×10^{16}	0.2720×10^{16}	-0.70	0.1350×10^{16}	0.1360×10^{16}	-0.74
0.375	0.1732×10^{16}	0.1737×10^{16}	-0.29	0.8655×10^{15}	0.8686×10^{15}	-0.36
0.400	0.1062×10^{16}	0.1057×10^{16}	+0.47	0.5306×10^{15}	0.5287×10^{15}	+0.36

*Data: 40 keV Boron Implant; Dose $5 \times 10^{11}\ cm^{-2}$; Drive-in Time = 1.0 hr; Inert Ambient (Argon) at 1000°C.

$$\% \text{ Error} \equiv \frac{\text{Numerical - Analytical}}{\text{Analytical}} \times 100$$

with the same window opening, that is, 2a = 1 μm, to calculate the initial distribution for a low dose ($5 \times 10^{11} cm^{-2}$) 40 keV arsenic implant according to Eq. (1). The resultant two-dimensional distribution, but with a uniform background $N_b = 10^{15} cm^{-3}$ subtracted from it, is shown in Fig. 5(a), while in Fig. 5(b) the equi-density contours are shown. For a drive-in time of 1 hr in an inert ambient (argon) at 1000°C, the redistributed two-dimensional arsenic profile and corresponding equi-density contours are shown in Figs. 6(a) and 6(b), respectively. The results shown in Fig. 6 were obtained by the analytical solution of Eq. (8) using a non-enhanced intrinsic diffusion coefficient of value 0.000615 $\mu m^2/hr$ for arsenic in silicon. Also, the computational domain $\{0 \leq x \leq L_o,\ 0 \leq y \leq b\}$ was reduced from that of the previous example by setting L_o and b equal to 0.25 μm and 0.75 μm, respectively. The reduction in these geometrical lengths was done such as not to impair the validity of the analytical solution given by Eq. (8). In the reduced computational domain, a fine ($\Delta x = \Delta y = 0.00625$ μm) partition was used and at each of the 21×61 grid points. Eq. (8) was used to obtain the analytical solution. The results for the numerical solutions shown in Fig. 7, which give the impurity concentration as a function of x for y = 0 μm and y = 0.5 μm (mask edge), were obtained using two rather fine partitions, that is $\Delta x = \Delta y = 0.0125$ μm and $\Delta x = \Delta y = 0.00625$ μm. An attempt was made to use the intermediate ($\Delta x = \Delta y = 0.025$ μm) and coarse ($\Delta x = \Delta y = 0.05$ μm) partitions which were used previously for the boron implant. However, they yielded numerical results that departed considerably from the analytical results, the reason being

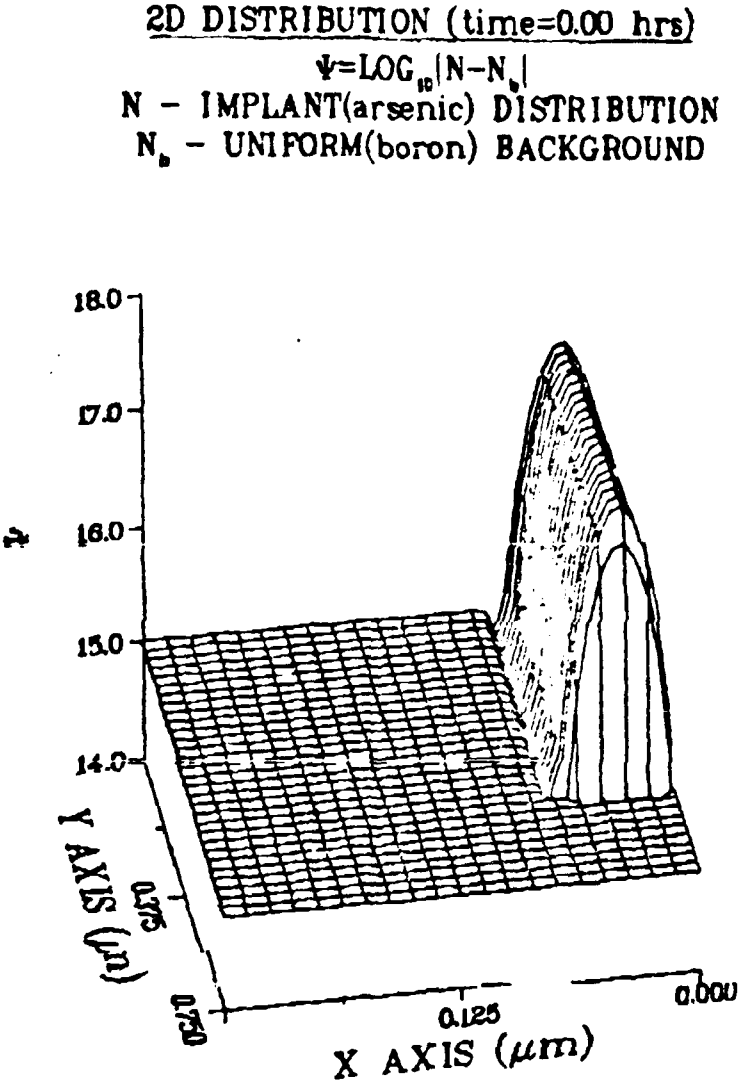

Fig. 5(a). Two-dimensional Furukawa distribution for a 40 keV arsenic implant of dose $5 \times 10^{11}\,cm^{-2}$.

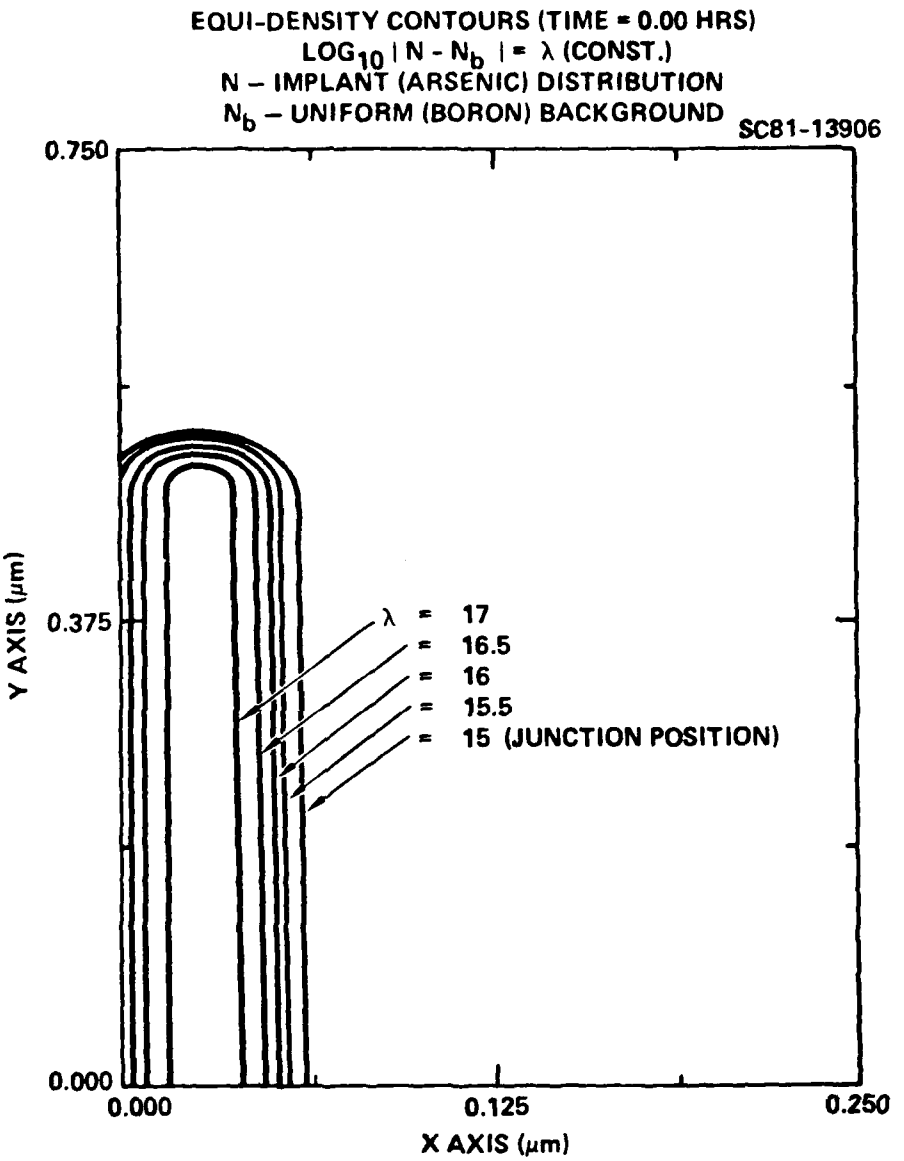

Fig. 5(b). The equi-density contours for Fig. 5(a).

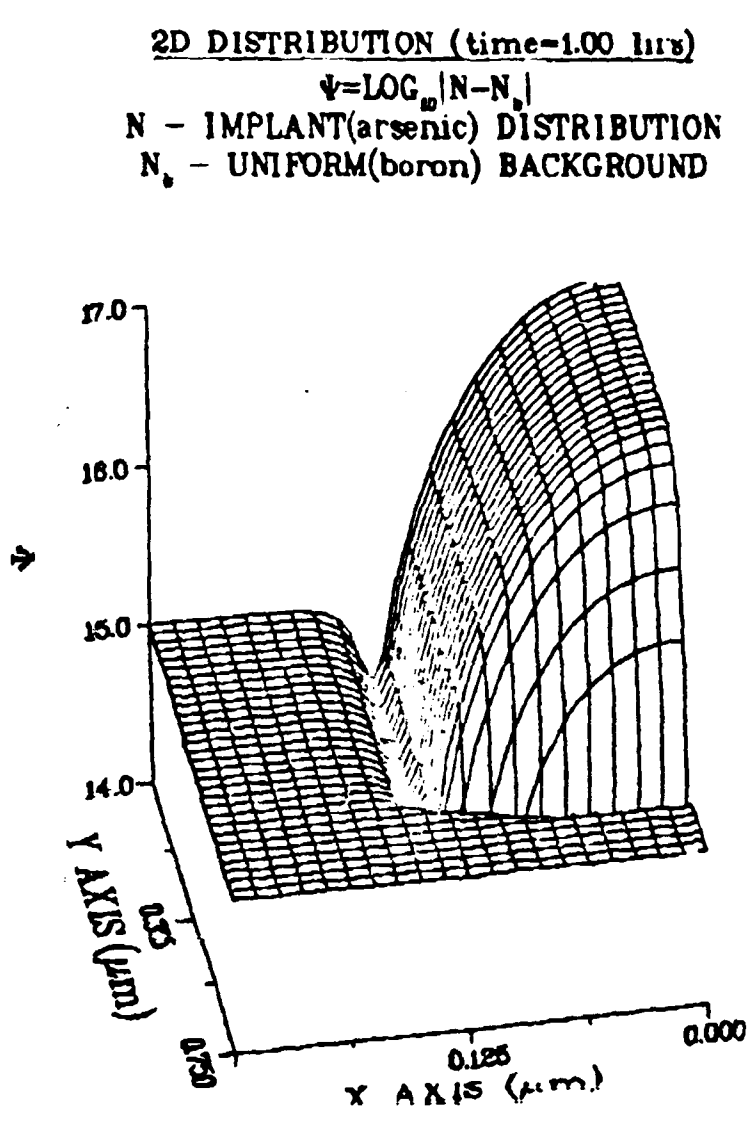

Fig. 6(a). Redistributed two-dimensional profile for the arsenic implant shown in Fig. 5 after 1 hr of drive-in time in an inert argon ambient at 1000°C.

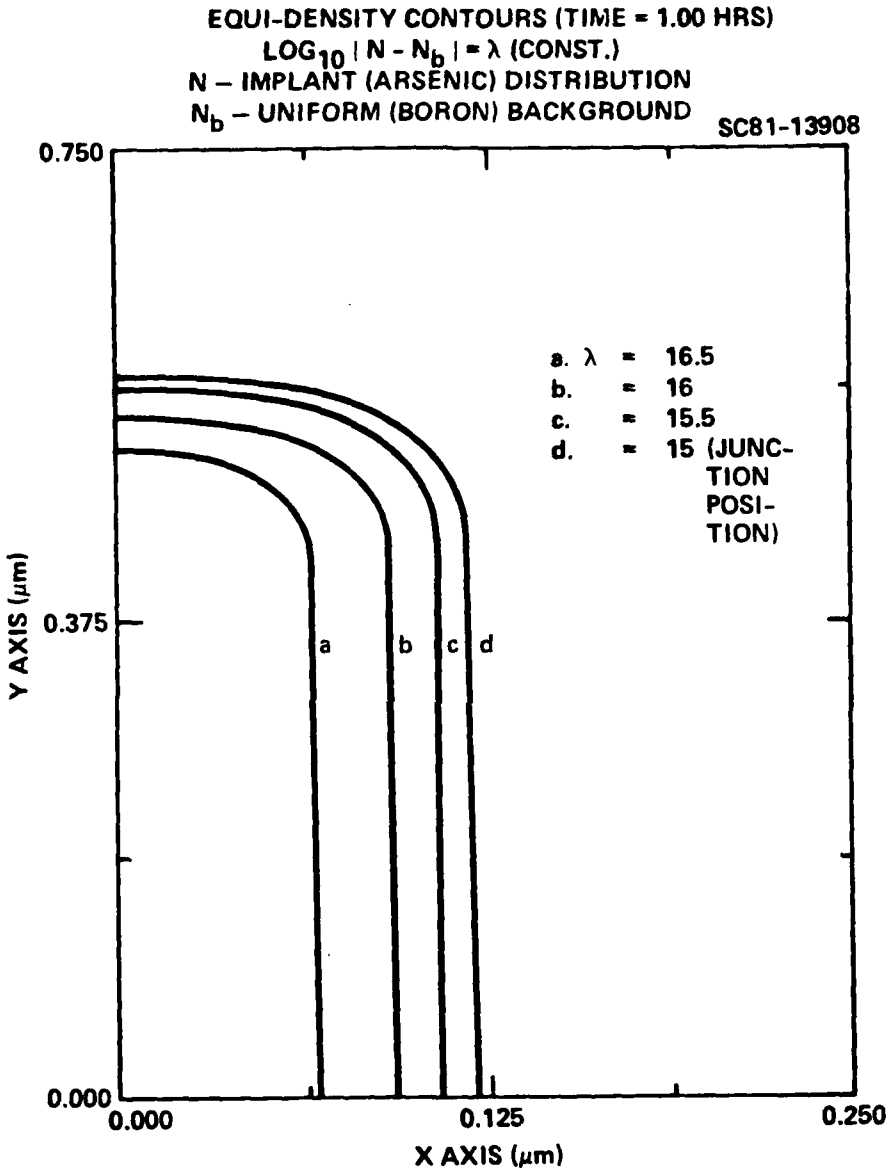

Fig. 6(b). The equi-density contours for Fig. 6(a).

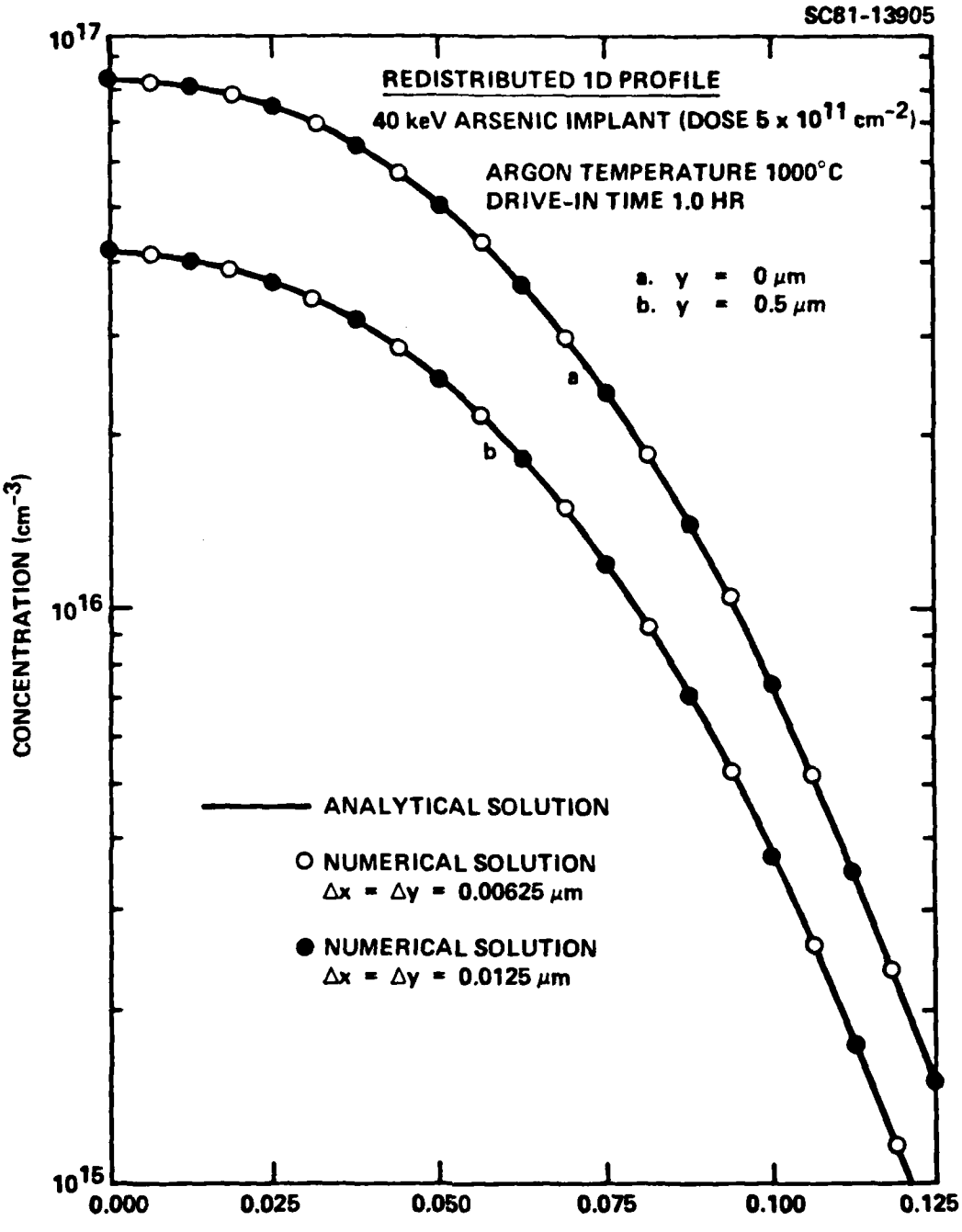

Fig. 7. Correlation of analytical and numerical predictions along the x direction for y = 0 μm and y = 0.5 μm (mask edge) for the distribution shown in Fig. 6, but with the redistributed implant decoupled from the background.

that with these cruder partitions, the initial two-dimensional distribution of the low energy 40 keV arsenic implant could not be characterized accurately because of the small σ_p and σ_L values.

An inventory of the results shown in Fig. 7 revealed that the numerical results for both partitions are in excellent agreement with the analytically predicted profiles. The quantitative correlation between the analytical and numerical results, where the latter utilizes the $\Delta x = \Delta y = 0.0125$ μm partition, is shown in Table 2.

Table 2. Correlation of Numerical and Analytical Predictions for Arsenic Implant*

x Position (μm)	y = 0 μm			y = 0.5 μm (Mask Edge)		
	Numerical (cm^{-3})	Analytical (cm^{-3})	% Error	Numerical (cm^{-3})	Analytical (cm^{-3})	% Error
0	0.8239×10^{17}	0.8299×10^{17}	-0.72	0.4128×10^{17}	0.4150×10^{17}	-0.53
0.01250	0.8035×10^{17}	0.8079×10^{17}	-0.55	0.4026×10^{17}	0.4039×10^{17}	-0.32
0.02500	0.7412×10^{17}	0.7423×10^{17}	-0.15	0.3713×10^{17}	0.3711×10^{17}	+0.05
0.03750	0.6380×10^{17}	0.6374×10^{17}	+0.09	0.3195×10^{17}	0.3187×10^{17}	+0.25
0.05000	0.5050×10^{17}	0.5054×10^{17}	-0.08	0.2527×10^{17}	0.2527×10^{17}	0.00
0.06250	0.3635×10^{17}	0.3659×10^{17}	-0.66	0.1817×10^{17}	0.1829×10^{17}	-0.66
0.07500	0.2366×10^{17}	0.2397×10^{17}	-1.29	0.1182×10^{17}	0.1198×10^{17}	-1.34
0.08750	0.1391×10^{17}	0.1411×10^{17}	-1.42	0.6941×10^{16}	0.7057×10^{16}	-1.64
0.10000	0.7393×10^{16}	0.7441×10^{16}	-0.65	0.3689×10^{16}	0.3721×10^{16}	-0.86
0.11250	0.3569×10^{16}	0.3503×10^{16}	+1.88	0.1780×10^{16}	0.1751×10^{16}	+1.66
0.12500	0.1572×10^{16}	0.1470×10^{16}	+6.94	0.7842×10^{15}	0.7348×10^{15}	+6.72

*Data: 40 keV Arsenic Implant; Dose $5 \times 10^{11} cm^{-2}$; Drive-in Time = 1.0 hr; Inert Ambient (Argon) at 1000°C.

$$\% \text{ Error} \equiv \frac{\text{Numerical - Analytical}}{\text{Analytical}} \times 100$$

3.0 REFERENCES

1. S. Furukawa, H. Matsumura, and H. Ishiwara, Japan J. Appl. Phys., Vol. II, pp. 134-142, 1972.

2. J.R. Lowney and R.D. Larrabee, IEEE Trans. Electron Devices, Vol. ED-27, No. 9, pp. 1795-1798, 1980.

3. J.F. Gibbons, W.S. Johnson, and S. Mylrose, "Projected Range Statistics," (Dowden, Hutchinson and Ross, Stroudsbourg, Pennsylvania, 1975).

APPENDIX

EFFICIENT NUMERICAL SOLUTION OF TWO-DIMENSIONAL NONLINEAR DIFFUSION EQUATIONS WITH NONUNIFORMLY MOVING BOUNDARIES: A VERSATILE TOOL FOR VLSI PROCESS MODELING*

W.D. Murphy and W.F. Hall
Rockwell International Science Center, Thousand Oaks, CA 91360

C.D. Maldonado
Rockwell International Microelectronics Research & Development Center
Anaheim, CA 92803

Abstract

A fast algorithm for the calculation of two-dimensional dopant redistribution during oxide growth has been developed. CPU times on the Cyber 176 are less than 30 seconds for the most computationally difficult process steps, including growth of a bird's beak field oxide. This represents a reduction in computer time of at least two orders of magnitude over techniques currently being employed, such as the B-spline finite element method used by Warner and Wilson[1]. Of greater significance is the fact that these CPU times are short enough to enable practical, iterative computer-based process design to be carried out in two dimensions.

The lateral diffusion of dopants between neighboring features on a silicon chip can no longer be ignored in the design of integrated circuit fabrication processes. Because the size and separation of features in VLSI circuits are comparable to the depths over which implants are to be redistributed, their resulting electrical characteristics are substantially affected by the spread of dopants into sensitive areas.

In the Stanford code SUPREM, the LSI process designer presently has at hand a powerful tool for predicting the effect of each process step on the vertical redistribution of dopants. Final dopant profiles can be generated in seconds on a fast computer such as the IBM 3033 or Cyber 176, enabling the designer to tailor the process quickly and easily for the desired result before expensive and time-consuming fabrication experiments are undertaken.

Our goal has been to provide comparable speed and flexibility for VLSI process design. Specifically, we have worked to develop fast algorithms for the calculation of two-dimensional dopant profiles resulting from VLSI fabrication processes, including nonuniform motion of the oxide-silicon boundary.

As a measure of our success, computer times of under 10 seconds have been achieved on the Cyber 176 for the generation of two-dimensional dopant profiles on a 21×41 grid for a 15-minute drive-in

*This work is supported in part by the Defense Advanced Research Projects Agency under Contract MDA903-80-C-0498.

cycle on boron-implanted silicon at 1100°C, with a peak initial boron concentration of 10^{20} cm^{-3}. This result can be directly compared with the work of Warner and Wilson[1], where similar nonlinear diffusion problems with the same number of unknowns, solved by second-order finite elements, took over 7 minutes on the Cray-1 computer. Since the Cray-1 is at least five times faster than the Cyber 176, this represents an improvement in speed by at least two orders of magnitude.

Dopant redistribution during high temperature process cycles is commonly described by diffusion of a single species with a concentration-dependent diffusivity. Ignoring diffusion in the oxide, which is justified in many cases, one can characterize the dopant redistribution problem as nonlinear diffusion in a bounded two-dimensional domain, with homogeneous boundary conditions at a (possibly) moving interface:

$$\frac{\partial N}{\partial t} = \nabla\cdot(D\nabla N) \ , \tag{1a}$$

$$\hat{n}\cdot D\nabla N = 0 \quad \text{at the silicon and sapphire boundaries} \ , \tag{1b}$$

$$\hat{n}\cdot D\nabla N = \hat{n}\cdot\hat{x}(k-m)(\partial U/\partial t)N \quad \text{at the oxide boundary} \ , \tag{1c}$$

where U is the local oxide thickness (along $\hat{x}$), k is the segregation coefficient, m is the ratio of silicon thickness consumed to oxide thickness produced, $\hat{n}$ is the unit normal at each boundary, N is the dopant concentration, and D is the diffusivity.

The geometry for our calculations models the growth of a bird's beak field oxide. The initial condition represents an ion implant, which is modeled by a Gaussian distribution in depth (x) and a complementary error function in the lateral dimension (y) about the mask edges, as suggested by Furukawa, *et al.*[2]. The rate of oxide growth is taken to vary locally in such a way that there is a smooth transition from the high growth rate on top of the field oxide to the low (or zero) growth rate under the mask. This is the general case for which our algorithms are developed; simple drive-in is obtained by immobilizing the oxide-silicon boundary.

The basic approach used in solving the nonlinear diffusion equation is the method of lines, coupled with the best currently available stiff integrator, GEARBI, of Hindmarsh[3]. This integrator is a variable order and variable step size method which is optimally first to fifth order accurate in time. To simplify the logic, the changing silicon region is mapped into a rectangle of constant dimensions, enabling a fixed computational grid to be used for the discretization and solution of the nonlinear diffusion equation as a system of ordinary differential equations.

Two types of mapping have been used: a scaling of the depth which varies with lateral position, and a conformal map whose level lines

approximate the oxide-silicon boundary shape. In the former case, cross derivatives appear in the differential equation and lateral derivatives appear in the boundary condition at the moving interface. Our preliminary investigations indicate that relatively fine meshes and tight error tolerance are required to produce acceptable solutions for this approach. In the latter case, these tolerances can be loose, but time is consumed in computing the mapping function and its derivatives. In either case, central differencing is used on the computational grid. The boundary conditions are incorporated by introducing "ghost" points immediately outside the computational domain whose values are determined from the discretized form of the boundary conditions.

The resulting set of coupled nonlinear ordinary differential equations $dN/dt = f(N,t)$ is stiff[4], and consequently an iterative procedure utilizing the Jacobian $\partial f/\partial N$ is required to converge the corrector equation in the linear multistep method used to integrate it. Most of the computer time is used in solving a large linear system $Px = b$ for the corrector, where the matrix P has the form $I - \mu\partial f/\partial N$. Consequently, it is critical that efficient methods be used in its solution. In GEARBI, a successive overrelaxation (SOR)[5] technique is employed, which is well suited to our problem because $\partial f/\partial N$ has only five nonzero nearest-neighbor diagonals. Other advantages of SOR are minimal storage requirements and, as P changes incrementally, fast convergence utilizing the previous solution for x as the initial iterate for the next time step.

CPU time and storage requirements are roughly linear with the number of equations being solved. This is a great improvement over banded matrix techniques, which require time and storage proportional to $L(M)^3$ and to $LM(3M+1)$, respectively, where L is the larger and M the smaller dimension on the computational grid. Furthermore, extensions to coupled species diffusion and to three spatial variables are easily accomplished with this software.

CPU times for all the cases we have run, including two-hour boron drive-in at 1000°C, are less than 30 seconds on the Cyber 176, using computational grids of up to 31×51 points. Results for the most general case of simultaneous diffusion and nonuniform oxide growth are illustrated in Figure 1. The conditions for this case model an 80 keV boron implant of 3×10^{13} cm^{-2} dose, oxidized in steam at 1000°C for half an hour. This problem was solved on a 31×51 grid in 12.5 seconds.

A typical drive-in problem without oxidation is illustrated in Figure 2. Here a high-dose 40 keV boron implant is redistributed over 2 hours at 1000°C. This problem required 22.5 seconds CPU time for a 21×31 grid.

Our primary objective in this effort is to provide the integrated circuits industry with a practical means of extending process design

to two dimensions. The algorithm described above meets this need. There remains, however, the task of incorporating these numerical methods into a complete process modeling code, after the fashion of SUPREM. We are presently engaged with the process modeling group at Stanford to achieve this end.

Acknowledgement

The authors wish to thank Dr. Alan Hindmarsh of the Lawrence Livermore Laboratory for suggesting and supplying his algorithm GEARBI.

References

1. D.D. Warner and C.L. Wilson, Bell Syst. Tech. J. 59, *1* (1980).

2. S. Furukawa, H. Matsumura, and H. Ishiwara, Japan J. Appl. Phys. *11*, 134 (1972).

3. Hindmarsh, A.C., "Preliminary Documentation of GEARBI," Lawrence Livermore Laboratory Report UCID-30149 (Livermore, California, 1976).

4. Gear, C.W., *Numerical Initial Value Problems in Ordinary Differential Equations*, Prentice-Hall (Englewood Cliffs, N.J., 1971).

5. Hageman, L.A., "The estimation of acceleration parameters for the Chebyshev polynomial and the successive overrelaxation iteration methods," Bettis Atomic Power Laboratory Report WAPD-TM-1038 (1972).

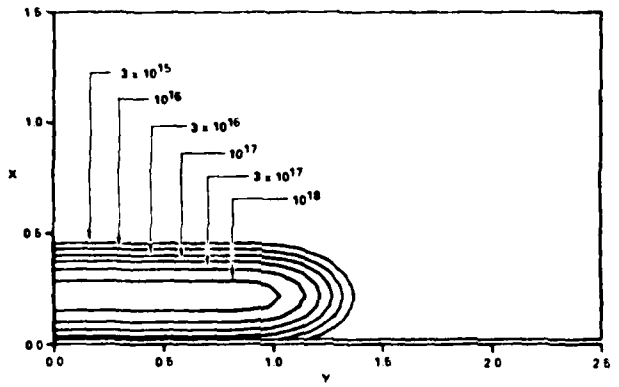

(a) Initial conditions after Furukawa, *et al.*[2].

(b) After 30 minutes in steam at 1000°C. Note motion of oxide boundary.

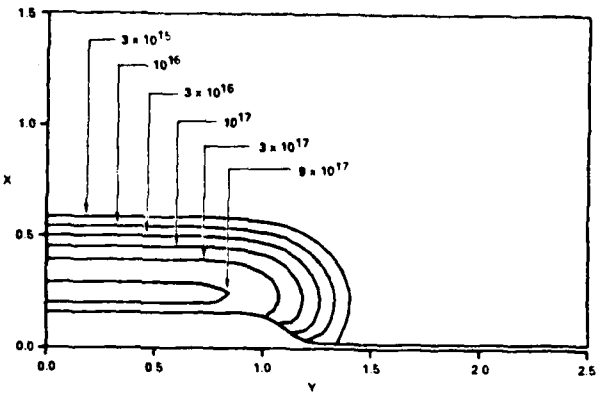

Fig. 1. Contours of constant dopant concentration.

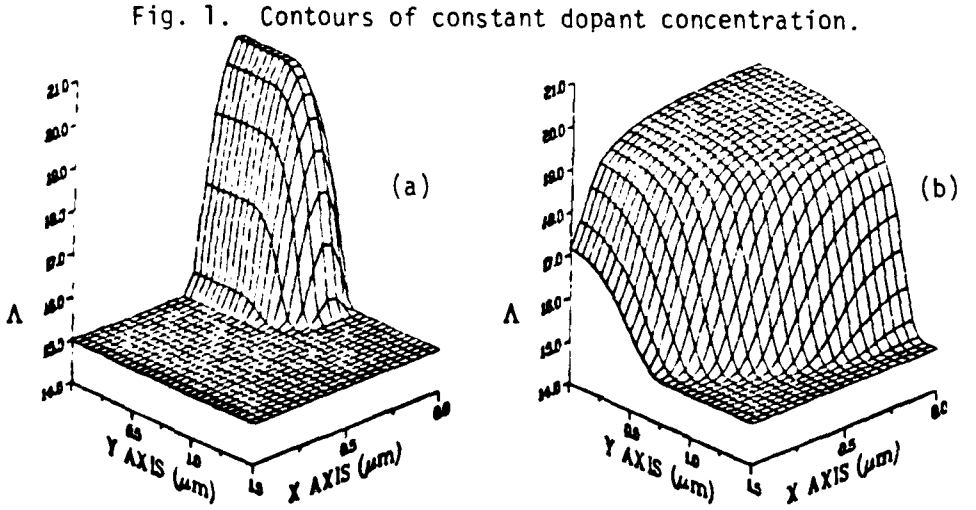

Fig. 2. Highly nonlinear diffusion of boron in silicon. Dose: $5 \times 10^{15}\,cm^{-2}$. Energy: 40 keV. $\Lambda = \mathrm{Log}_{10}\,|N + N_b|$. Temperature = 1000°C. (a) Initial concentration profile (time = 0). (b) Dopant profile after one hour.

2D PROCESS MODELING AND SIMULATION FOR VLSI DESIGN*

C. D. Maldonado, ** W. F. Hall, † W. D. Murphy, † and S. A. Louie**

Rockwell International Corporation
Anaheim, CA

ABSTRACT

The nonlinear and *nonuniform moving* boundary value problem which governs the redistribution of a field implant during the growth of a bird's beak, is formulated and solved by a highly efficient numerical algorithm. The formulation is sufficiently general so as to be applicable to SOS and bulk device geometries. It is also shown that every other redistribution problem encountered in the fabrication of VLSI devices is a special case of the field implant redistribution problem.

*This work was supported in part by the Defense Advanced Research Projects Agency under Contract MDA903-80-C-0498.
**Rockwell International Microelectronics R&D Center, Anaheim, California.
†Rockwell International Science Center, Thousand Oaks, California.

2D PROCESS MODELING AND SIMULATION FOR VLSI DESIGN*

C. D. Maldonado,** W. F. Hall,† W. D. Murphy,† and S. A. Louie**

Rockwell International Corporation

Anaheim, CA

SUMMARY

As device geometries are reduced in size the use of two dimensional (2D) device and process simulators as design aids will become increasingly important. Two dimensional device simulators have been successfully developed during the past decade but at the present time no 2D process simulator similar to the 1D process simulator, SUPREM[1], exists. In a recent series of papers [2]-[4], the nonlinear boundary-value problem which governs the redistribution of implants under nonoxidizing conditions, is solved numerically by different algorithms. An exact analytical solution to this same problem but for low dose implants, has been obtained by Lee et. al [5]. Also, approximate analytical solutions have been obtained [6], [7] to predict the redistribution of low dose implants under oxidizing conditions. In all these two dimensional redistribution problems the semiconductor medium is semi-infinite in extent in the vertical direction (bulk device type geometry).

The present trend in VLSI technology is to fabricate devices entirely by ion implantations, like the NMOS enhancement mode device shown in Figure 1. The final 2D profiles that are obtained after the device fabrication schedule is completed, represent important information for accurate electrical device characterization. The problem of determining the redistribution of a field implant is pertinent since every other redistribution problem is a special case of it. Therefore, if an efficient numerical algorithm can be developed to solve the field implant redistribution problem then all the tools which are necessary to assemble a SUPREM-like 2D process simulator, will be readily available.†† It is the purpose of this paper to formulate, numerically solve, and apply the resultant solution to predict the redistribution of a field implant. Special cases pertaining to the redistribution of source/drain and enhancement mode channel implants are also considered.

The initial SOS geometry for defining the field implant redistribution problem is shown in Figure 2(a). Because the device is symmetrical about the y=0 position, only the shaded region of Figure 2(a) is used in formulating the problem. The window opening ($|y| \leq a$) in the impenetrable mask allows the field implant to penetrate the initial thin oxide layer and distribute itself within the semiconductor medium in a two-dimensional manner [8]. When the photoresist portion of the impenetrable mask is removed and the resultant structure brought into contact with an oxidizing environment the growth of a field oxide will take place with a lateral penetration of the bird's beak under the mask edge as shown in Figure 2(b). Applying conservation and continuity arguments to the impurity concentration together with the assumption that Fick's law [9] is applicable, we derive the governing boundary value problem for the redistribution of a field implant in the shaded region of Figure 2(b). For high dose implants the boundary value problem is highly nonlinear due to the diffusion coefficient's dependence on impurity concentration.

Besides being nonlinear for high dose implants, the boundary value problem is further complicated by the fact that the boundary between the oxide and semiconductor media is moving nonuniformly as a function of time and lateral position. To solve this boundary value problem numerically in a highly efficient manner the shaded region in Figure 2(b) which is decreasing in time, is transformed to the stationary rectangular shaded region of Figure 2(c). This mapping was achieved by a translation-scaling transformation. The stationary rectangular shaded region was subdivided uniformly in both the ξ and η directions. On the resultant computational grid the classical method of lines was used to discretize the transformed boundary value problem into a stiff system of coupled ordinary nonlinear differential equations. The resultant system of equations was then solved by utilizing the best currently available stiff integrator, GEARBI, of Hindmarsh [10]. This integrator is a variable order and variable step size method which is optimally first to fifth order accurate in time. Also, in GEARBI, a successive over-relaxation (SOR) [11] technique is employed, which is well suited to the present problem because the Jacobian has only five nonzero nearest-neighbor diagonals. A detail discussion on the numerical technique is presented elsewhere [12].

The computer program based on the numerical algorithm of reference [12] was utilized to predict the redistribution of an 80 keV boron field implant of dose 3×10^{13} cm^{-2} during the growth of a field oxide using an oxidizing ambient of steam at 1000°C for 2.333 hours. The resultant equi-concentration contours are shown in Figure 3. Likewise, the computer program was applied to the special cases corresponding to the redistribution of source/drain and channel implants and the results for the equi-concentration contours are shown in Figures 4 and 5, respectively. Figure 4 is for the redistribution of a channel profile which is composed of a shallow 40 keV boron implant (dose 2×10^{11} cm^{-2}) superimposed on a deep 120 keV boron implant (dose 1.5×10^{11} cm^{-2}), during the growth of a gate oxide by an oxidizing ambient of steam at 1000°C for 0.25 hour. In Figure 5 the redistribution is for a high dose 5×10^{15} cm^{-2} (source/drain) 40 keV arsenic implant which is being driven-in by a nonoxidizing ambient of argon at 1000°C for 1 hour.

The results of Figures 3, 4, and 5 were based on the concentration dependent diffusion coefficient of Warner and Wilson [2]. For the results of Figure 3 the oxide growth model of Deal and Grove [13] was modified empirically to characterize the lateral position and time dependence of the bird's beak. Computations were carried out on the CDC cyber 176 computer. To illustrate the computational efficient of the numerical algorithm examples of grid size and the resultant computational times for all three redistribution problems considered in this paper are presented in Table I.

*This work was supported in part by the Defense Advanced Research Projects Agency under Contract MDA903-80-C-0498.

**Rockwell International Microelectronics R&D Center, Anaheim, California.

†Rockwell International Science Center, Thousand Oaks, California.

††Presently, we are collaborating with the process modeling group at Stanford University to develop a 2D process simulator similar to SUPREM.

REFERENCES

[1] D A Antoniadis, S E Hansen, and R W Dutton, "SUPREM II – A Program for IC Process Modeling and Simulation," TR No 5019-2 Stanford Electronics Laboratories, Stanford University, Stanford, Calif 1978

[2] D D Warner and C L Wilson, *Bell Sys Tech J*, Vol 59, pp 1-41, 1980

[3] R Tielert, *IEEE Trans Electron Devices* Vol ED-27, No 8, pp 1479-1483, 1980

4 H Ryssel et al, *IEEE Trans Electron Devices* Vol ED-27, No 8, pp 1484-1492, 1980

5 H G Lee, J C Sansbury, R W Dutton, and J L Moll, *IEEE J Solid State Circuits* Vol SC-13, pp 455-561, 1978

6 H G Lee, "Two-Dimensional Impurity Diffusion Studies Process Models and Test Structures for Low-Concentration Boron Diffusion," TR No 6201-8 Stanford Electronics Laboratories, Stanford University, Stanford Calif 1980

7 D J Chin, M R Kump, H G Lee, and R W Dutton, "Process Design Using Coupled 2D Process and Device Simulators" presented at the International Electron Devices Meeting, Washington D C, Dec 8-10, 1980

[8] S Furukawa, H Matsumura, and H Ishiwara, *Japan J Appl Phys* Vol 11, pp 134-142, 1972

[9] J R Lowney and R D Larrabee, *IEEE Trans Electron Devices*, Vol ED-27, No 9, pp 1795-1798, 1980

[10] A C Hindmarsh, "Preliminary Documentation of GEARBI," Lawrence Livermore Laboratory Report UCID-30149, Livermore, Calif 1976

[11] C W Gear, Numerical Initial Value Problems in Ordinary Differential Equations, *(Prentice-Hall, Englewood Cliffs, N.J., 1971)*

[12] W D Murphy, W F Hall, and C D Maldonado, "Efficient Numerical Solution of Two-Dimensional Nonlinear Diffusion Equations with Nonuniformly Moving Boundaries A Versatile Tool for VLSI Process Modeling," to be presented at the Second International Conference on the "Numerical Analysis of Semiconductor Devices and Integrated Circuits" Trinity College Dublin, Ireland, June 17-19, 1981

[13] B E Deal and A S Grove, *J Appl Phys*, Vol 36, No 12, pp 3770-3778, 1965

Table 1. Grid Size and Computational Time*

RESULTS	GRID SIZE	TIME
Figure 3	31 x 51	22 sec
Figure 4	41 x 81	33 sec
Figure 5	41 x 61	42 sec

*CDC Cyber 176 Computer

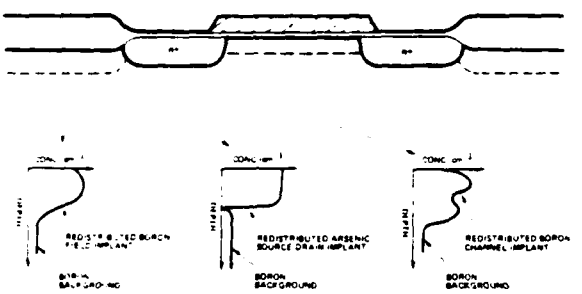

Figure 1. Qualitative 2D geometrical sketch of an NMOS enhancement mode device with final redistributed profiles for the field, source/drain, and channel implants.

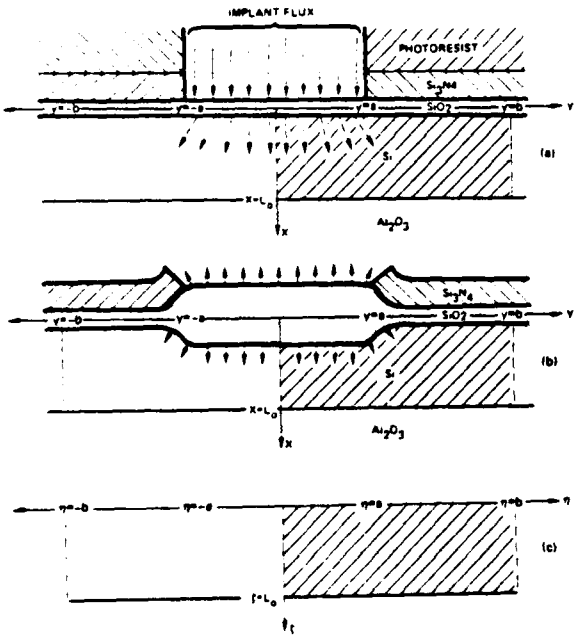

Figure 2. Initial SOS geometry and corresponding transformed geometry that takes place during the growth of a field oxide are shown in (a) and (b), respectively; while in (c) is shown the stationary rectangular (shaded region) computational domain in the transformed (ξ, η) coordinate system.

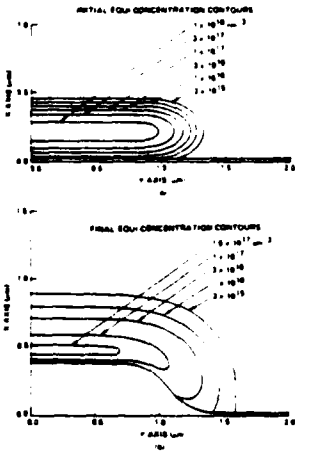

Figure 3. Initial and final equi-boron concentration contours for the redistribution of a field implant are shown in (a) and (b), respectively.

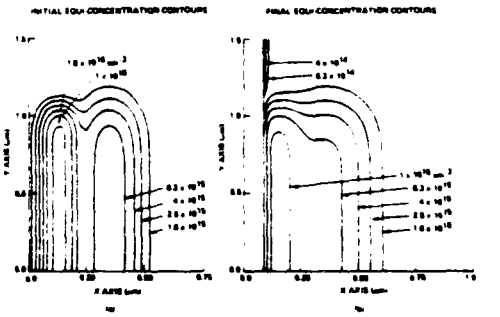

Figure 4. Initial and final equi-boron concentration contours for the redistribution of a channel enhancement mode profile are shown in (a) and (b), respectively.

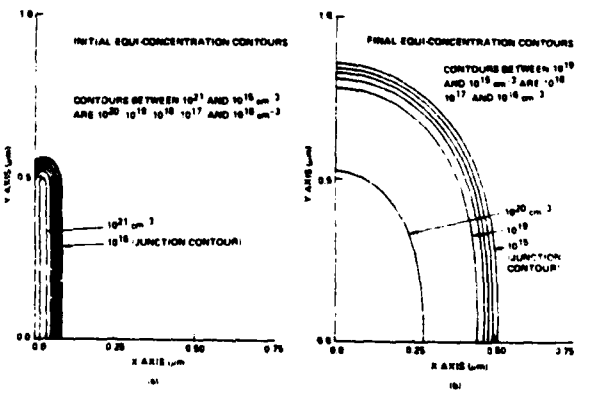

Figure 5. Initial and final equi-arsenic concentration contours for the redistribution of a source/drain implant are shown in (a) and (b), respectively.